Mechanical and Optical Characterization of a Photoviscoplastic Material

JAMES F. DOYLE, *School of Aeronautics and Astronautics, Purdue University, West Lafayette, Indiana 47907*

Synopsis

The mechanical and optical properties of a polyester blend over a wide range of strain rates has been investigated for loading and unloading. The mechanical behavior, while being complex, was modeled adequately with a generalization of the four-parameter viscoelastic model. The optical behavior has at least a three-phenomenological coefficient dependence on the mechanical variables. Further, the stress birefringence is of opposite sign to that of the deformation.

INTRODUCTION

Structural materials are being used in more sophisticated ways than ever before, and a need has arisen for the development of experimental methods for their analysis in these situations. A case in point is the design for impact loading; here, not only is the structural response very different from the static case but the material response may also be very different. Photoelasticity has proved very successful for the nominally linear-elastic problems, and it is only natural that attempts are made to extend this optical method to the nonlinear or time-dependent materials.

Photoelasticity is a model method in the sense that the structural material is replaced by another with the same mechanical response to load but, in addition, with the desirable optical properties. These model materials are invariably polymeric, and for this reason the investigation of polymers plays an essential role in the development of the method.

Unfortunately, the search for suitable materials for the nonlinear analysis has not been very successful, and a review of some of the materials tried is given in reference 1. The purpose of the present paper is to report on a model material for use in problems involving large strain rates and where the unloading behavior is deemed to be of importance.

EXPERIMENTAL TESTING

A material shown to have good potential use[1–3] is a polyester blend because it is possible, by varying the mixtures, to obtain a material with any desired stress–strain response. It was therefore chosen for further study. The particular mix investigated was an 80/20 ratio per weight of Paraplex P-13 and Paraplex P-43 (flexible and rigid, respectively) with 1% benzoyl peroxide as catalyst, to give a tough, flexible material. Sheets nominally 300 × 300 × 8 mm were cast by a combination of methods,[1–4] and their mechanical and optical properties seemed reproducible from batch to batch.

Journal of Applied Polymer Science, Vol. 24, 1295–1304 (1979)

0021-8995/79/0024-1295$01.00

The testing was divided into two main parts; low strain rates (LSR) which range from $\dot{e} = 10^{-5}$ to 10^{-1} strain/sec, and high strain rates (HSR) where $\dot{e} = 10^2$ to 10^4 strain/sec and corresponds to impact. All these tests were carried out under uniaxial stress conditions, and only for the LSR tests was the complete loading/unloading behavior of the material monitored.

The LSR tests were performed on a Universal testing machine and were run at essentially constant head rate up to a preassigned value of extension. The loading then reversed, and unloading proceeded at the same rate until zero load. Recovery information was inferred by following the head movement in order to maintain zero load in the specimen. In retrospect, however, a separate series of recovery and creep tests should also have been performed. For the slower rates, transverse measurements were made so as to estimate the static Poisson ratio. The optical setup was a circular polariscope with a mercury arc light source, and the birefringence intensity variation was recorded by focusing the image of the specimen onto a photometer. The extension, load, and birefringence were recorded with respect to time on an x–y plotter. Twelve complete tests were performed (some were repeats so as to check consistency of the different batches) at an ambient temperature of 28°C, and sample histories are shown in Figure 1. The material exhibits sizable rate effects. After unloading, some but not all of the deformation is recovered. The optical data are interesting because for a given small deformation the lower rate shows a higher fringe value, which indicates that the stress optic effect is of opposite sign to that of the deformation. But for a given large deformation the higher rate shows a higher fringe value, indicating the presence of some other optical effect. The proportion of a given deformation that is permanent is smaller at the higher rates, and this may be the parameter that accounts for the difference, if it is less optically sensitive than the elastic component. For example, for the two specimens shown in Figure 1, the difference in birefringence as a function of strain is given as

Strain	0.04	0.08	0.12	0.16	0.20	0.225
Difference in birefringence	0.045	0.14	0.18	0.17	0.12	0.06

If the strain of Model 2L had been taken to a larger value, then it would be more obvious that for a given large strain, the high rate data show the larger value of birefringence. The above data, nonetheless, show this trend.

A special Split Hopkinson Pressure Bar (SHPB) apparatus was built in order to perform the HSR tests. The design is shown in Figure 2 and is basically that of reference 5. This particular system used a three-gauge arrangement, and typical oscilloscope outputs are shown in Figure 3. The light source of the optical setup was a 1-mW HeNe laser beam expanded to about 1.5 mm in diameter at the model. The variation of light was picked up by a MRD500 pin silicon photodiode and displayed on the oscilloscope. While no anomalous dispersion was detected during LSR testing, judging in retrospect it would have been preferable to use the laser light source for both sets of data.

The specimens were nominally 8 mm square in cross section, and the length ranged from 3 to 10 mm. Many specimens were tested but only nine were completely analyzed. A small computer program was written to convert the oscilloscope traces to stress, deformation, and birefringence histories, and some sample histories are shown in Figure 3. The optical data follow closely those of the stress, which shows that they are primarily stress dependent; but in cases

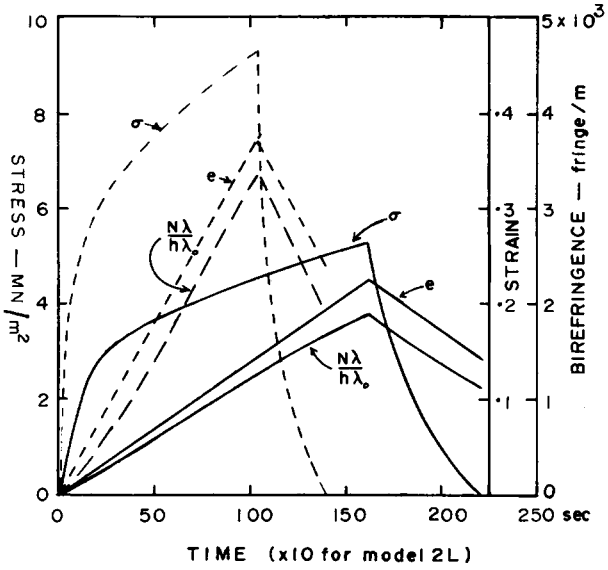

Fig. 1. Typical mechanical and optical histories: (- - -) model 4S; (—) model 2L.

where the stress remained essentially constant, the fringe order decreased even though the deformation continued to increase. This confirms the expectation that the stress birefringence is opposite that of the deformation.

CONSTITUTIVE RELATION

A preliminary analysis indicates that the material is not one of the simple types such as viscoelastic or elastic–plastic. There is also no apparent simple relationship between the birefringence and either the stress or the strain. A full mechanical characterization is therefore essential before the optical effect can be described.

It is noted that the material exhibits the following characteristics: it is time dependent, has a rate-dependent initial modulus, suffers permanent deformations (at all levels of stress), has a rate-dependent yield stress, and has some recovery ability. The mechanical model which exhibits (in a linear manner) all of these is the Maxwell model in series with a Kelvin model. Such a model has been suitably generalized[6] for three-dimensional, nonlinear behavior and put in a form that satisfies the requirement for a proper statement of a constitutive relation. A special case, one that is not too obtuse, takes on the following form for uniaxial stress:

$$d_{xx} = -K\left[E^e_{xx} - \left(\frac{1-2\nu}{3E}\right)\sigma\right] + \frac{\dot{\sigma}}{\tilde{E}} + [\Phi + \Psi]\frac{2}{\sqrt{3}}$$

$$d_{yy} = -K\left[E^e_{yy} - \left(\frac{1-2\nu}{3E}\right)\sigma\right] - \frac{\dot{\sigma}}{3\tilde{E}} - [\Phi + \Psi]\frac{2}{\sqrt{3}}$$

$$\tilde{E} = \frac{3E}{(1-2\nu) + (1+\nu)2\Omega} \tag{1}$$

where E_{xx} is the total strain, i.e., the sum of E^e_{xx} and E^p_{xx}; d_{xx} is the deformation

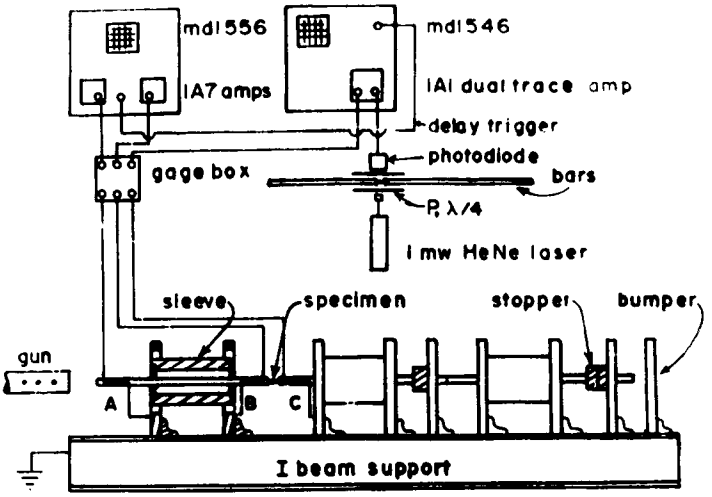

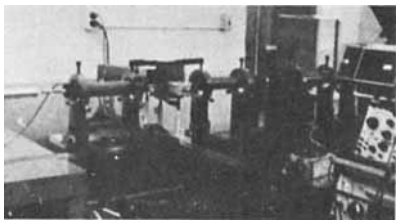

Fig. 2. Layout and design of SHPB apparatus.

rate (which for small strains is the same as $\dot{E}_{xx}$); σ is the stress; and E and ν are coefficients which in the rate-independent case have the meaning of Young's modulus and Poisson's ratio, respectively. The functions K, Ω, Φ, and Ψ are empirical and chosen to best fit the experimental data. The major effects of these are: K governs the recovery ability, Ω determines dependence of the initial modulus on the deformation rate and stress, Φ governs the viscous rate of deformation, and Ψ governs the rate of permanent deformation.

The functions Φ and Ψ determine the "yielding" of the material, that is, the stress level beyond which there is a rapid onslaught of viscous or permanent effects. They are functions of the invariants of stress and strain, in particular of the second invariants of the deviatoric stress and strain, and denoted as $\mathbf{J}_2$ and $\mathbf{I}_2$, respectively. The volumetric relation is assumed to be linear and rate independent because it is generally found that polymers are viscous in shear but ideally elastic in dilation.[7]

For short times,

$$\frac{d\sigma}{dE_{xx}} = \tilde{E}_0 = \frac{3E}{(1-2\nu)+(1+\nu)2\Omega} \tag{2}$$

$$-\frac{dE_{yy}}{dE_{xx}} = \tilde{\nu}_0 = \frac{(1+\nu)\Omega_0 - (1-2\nu)}{(1+\nu)2\Omega_0 + (1-2\nu)} \tag{3}$$

That is, the initial Young's modulus $\tilde{E}_0$ and Poisson's ratio $\tilde{\nu}_0$ may be rate dependent through Ω.

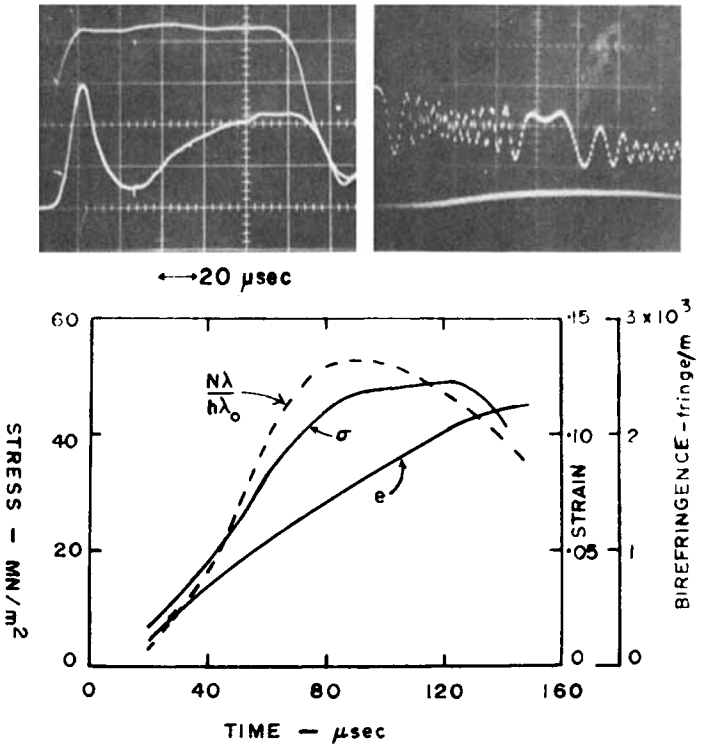

Fig. 3. Typical dynamic history.

To construct an optical constitutive relation, it is of value to recall the mechanical model for the deformation of polymers. Here, the deformation is comprised of instantaneous elasticity, retarded elasticity, and permanent deformations. It is assumed that there are definite physical events occurring in the molecule chains that can be associated with each of the three types of deformation proposed by that model. It is further assumed that all of these will have their separate contribution to the dielectric tensor. There may of course be other contributions, but these three are assumed to be the dominant ones. The optical constitutive relation may be shown[6] to reduce to

$$N\frac{\lambda}{h}\begin{Bmatrix}\cos 2\theta\\ \sin 2\theta\end{Bmatrix} = C_\sigma\begin{Bmatrix}\sigma_{xx}-\sigma_{yy}\\ 2\sigma_{xy}\end{Bmatrix} + C_e\begin{Bmatrix}E_{xx}-E_{yy}\\ 2E_{xy}\end{Bmatrix}^e + C_p\begin{Bmatrix}E_{xx}-E_{yy}\\ 2E_{xy}\end{Bmatrix}^p \quad (4)$$

where N is the observed fringe order and θ is the observed isoclinic angle.

The optical coefficients C_σ, C_e, and C_p are empirically determined and may be functions of any of the mechanical invariants. This optic law, which is simple in appearance, can be shown to represent many diverse birefringent phenomena ranging from viscoelasticity to elastoplasticity to viscous flow.[8] A discussion of all its implications is very interesting but beyond the scope of this paper.

MATERIAL CHARACTERIZATION

In the data reduction, the current area and thickness are estimated by assuming no volume change, giving respectively

$$A = \frac{A_0}{1+e}, \qquad h = \frac{h_0}{\sqrt{1+e}}$$

This approximation is considered acceptable since a static value of Poisson's ratio of $\nu = 0.47$ was obtained from the transverse measurements. The extension e is a suitable parameter in which to express the data, since all the strain measures needed are simply related to it. Ideally, all the coefficients should be obtained simultaneously, but it is convenient to associate them with different stages of the deformation and to evaluate them there. If greater accuracy is required, then the procedure can be iterated.

The initial modulus is very rate dependent, as shown in Figure 4(a), and the particular argument of dependence was chosen so as to give a definite limit at low rates. This limit was taken as E, the static Young's modulus. For simplicity Ω is assumed to be a function only of the deformation rate and is obtained from

$$\left(\frac{1+\nu}{E}\right)\Omega = \frac{3}{2\tilde{E}_0} - \left(\frac{1-2\nu}{2E}\right), \qquad \tilde{E}_0 = E[1 + a \log_e(1 + 10^4 \mathbf{I}_2{}^{d1/2})] \tag{5}$$

where a is an empirical constant, $\mathbf{I}_2{}^d$ is the second invariant of the deformation rate tensor. The recovery coefficient K is nonlinear, and Figure 4(b) shows its dependence on the level of strain. The viscous on-flow parameters Φ and Ψ are taken in the form

$$\Phi,\Psi = [\mathbf{J}_2/k]^b = d_{xx}^{ve}, \qquad d_{xx}^{vp}, \qquad k = k(\mathbf{I}_2^{1/2}) \tag{6}$$

Figure 5 shows a sample variation of the parameters with strain rate.

Using the evaluated coefficients, the constitutive equations were integrated using the experimental stress histories; Figure 6 shows a comparison of some of the stress deformation diagrams. All in all, the mechanical model is considered satisfactory since it is capable of describing the material's dominant characteristics of rate-dependent initial modulus, viscous flow, recovery, and permanent deformation for both loading and unloading within a wide range of rates.

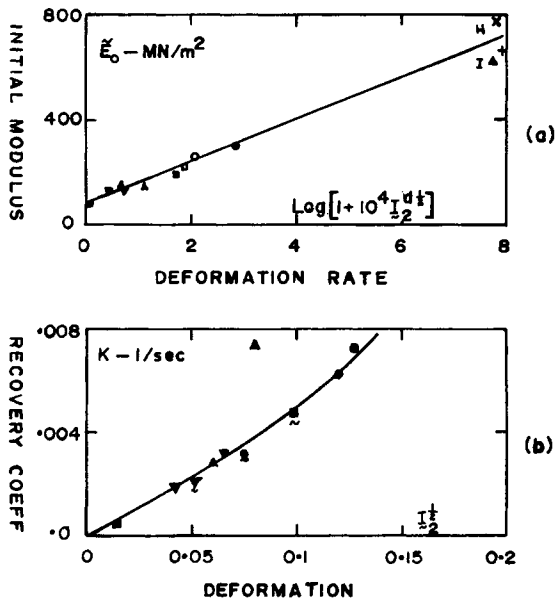

Fig. 4. (a) Variation of initial modulus with deformation rate. (b) Dependence of recovery coefficient on deformation.

The fringe history data are normalized by putting it into $N\lambda/h\lambda_0$ form, where the reference wavelength λ_0 is taken as 546 nm. The general form of the optical equation for uniaxial stress is written as

$$\frac{N\lambda}{h\lambda_0} = C_\sigma + \frac{3}{2}C_e\left[E_{xx} - \frac{1-2\nu}{3E}\sigma\right] + \frac{3}{2}[C_p - C_e]E^p_{xx} \tag{7}$$

because it makes it easier to handle. In general, the coefficients may be functions of the mechanical invariants, but here they are assumed constant. This is a three-coefficient relation, and it is difficult to display it on a two-dimensional plot so as to evaluate the coefficients. The manner of plotting the data chosen in Figure 7, however, greatly aids this task.[10] If the data follow a straight line, then (i) there is little permanent deformation effect, (ii) the slope is the stress optic coefficient, and (iii) the vertical intercept is the strain optic coefficient. If there are permanent deformation effects, then the data will deviate from a straight line.

Figure 7(a) shows a plot of the data at low rates assuming that the permanent deformation has no special effect. The data as a whole appear totally random,

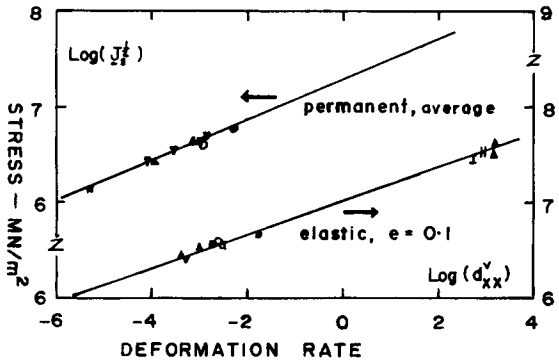

Fig. 5. Dependence of viscous deformation rate on stress.

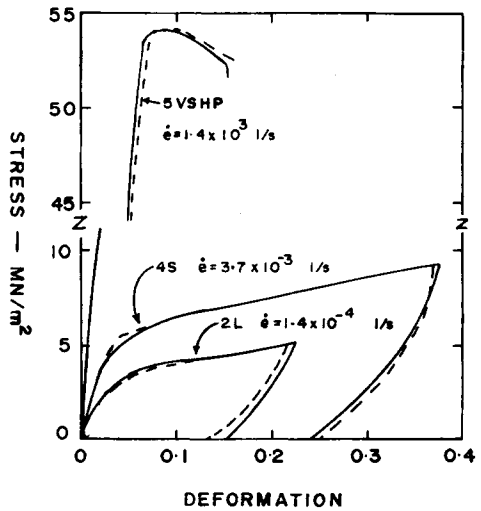

Fig. 6. Comparison of stress–deformation diagrams: (—) experimental; (- - -) model.

but if they are followed for each model then there is some correlation; they show a negative, nearly linear dependence on stress that is the same for each model. The deformation coefficient (vertical intercept), however, is different in each case, and the recovery data do not tie in at all. Figure 7(b) shows the optical response at high rates (where permanent deformation is negligible), and the same dependence on stress is obtained. This firmly establishes that the stress optic coefficient is of opposite sign to that of the deformation. Improved correlation is obtained (even for the recovery data) when the permanent deformation is assumed to have its own separate contribution to the optical effect. When all the coefficients are obtained simultaneously, they are found to be

$$C_\sigma = -53.4 \text{ fringes} \cdot \text{m/MN}, \qquad C_e = 8095 \text{ fringes/m},$$

$$C_p = 3673 \text{ fringes/m}$$

and Figure 8 shows a comparison of the maximum fringe value obtained experimentally with that predicted by the model. The agreement is reasonable, especially when the amount of data reduction involved is considered.

The assigning of the negative sign to the stress optic coefficient is arbitrary and is used only to signify that it is opposite to that of the deformation If does not necessarily correspond with the convention set up in such works as that of Javornicky.[11] Parenthetically, it may be noted that such works have shown the existence of materials with birefringent components of opposite sign.

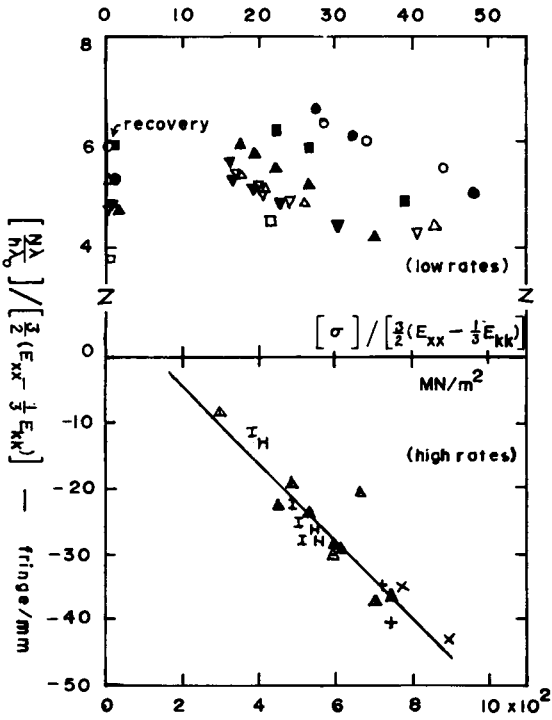

Fig. 7. Birefringence at low and high rates.

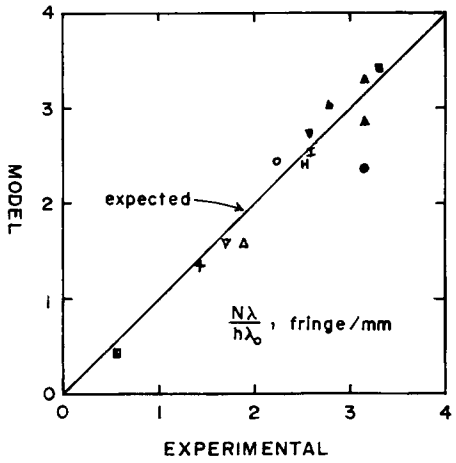

Fig. 8. Comparison of maximum experimental and modeled birefringence reached.

CONCLUSIONS

The mechanical properties of polyester blends are very complicated, and complex models must be used to describe their behavior. This is especially true if unloading is considered. The optical response is tied in closely with the mechanical behavior, so it too is very complicated. Indeed, the present data indicates that the optical response has at least a three-phenomenological coefficient dependence on the mechanical variables and that the respective contributions are not necessarily of the same sign.

A similar material was used by Weiss et al.[1] and Chase and Goldsmith,[9] but with a different approach to optical characterization. In fact, a rate-dependent strain optic relation was used and the conclusion drawn that this material is suitable for dynamic photoplastic studies. The present work, however, shows that there are certain combinations of stress and deformation for which the fringe values will change sign. This makes fringe interpretation highly ambiguous, and therefore it must be concluded that this material is unsuited for dynamic photomechanics. The reason for the different conclusions appears to lie in the fact that the material of the above studies[1,9] was optically calibrated for very large strains and strain rates only up to 100 strains/sec. Both of these tend to obscure the stress dependence. However, the usual situation during impact is large stresses for very short periods of time (and hence small strains), causing the optical effect to be dominated by the stresses.

References

1. R. T. Weiss, K. Chase, and W. Goldsmith, *J. Polym. Sci. A-2*, 8, 1713 (1970).
2. D. Henley, T&AM Report #335, University of Illinois, 1967.
3. D. Morris and W. F. Riley, *Exp. Mech.*, December 1972, pp. 448–453.
4. D. Morris, *Exp. Mech.*, June 1975, p. 19N.
5. S. Chou, K. D. Robertson, J. H. Rainey, AMMRC, TR 71-49, Nov. 1971.
6. J. F. Doyle, T&AM Report #420, University of Illinois, September 1977.
7. S. R. Bodner and Y. Partom, *J. Appl. Mech.*, 385 (1975).
8. J. F. Doyle, *Exp. Mech.*, November 1978, pp. 416–420.
9. K. Chase and W. Goldsmith, *J. Appl. Mech.*, 63 (1974).

10. J. F. Doyle, *Exp. Mech.* to appear.
11. J. Javornicky, *Photoplasticity*, Elsevier, Amsterdam, 1974, pp. 84–92.

Received October 10, 1978
Revised March 27, 1979